

ELECTROCHEMICALLY SYNTHESIZED Si NANOWIRE ARRAYS AND THERMOELECTRIC NANOSTRUCTURES

Ng Inn Khuan*, Kok Kuan Ying, Nur Ubaidah Saidin and Choo Thye Foo

Material Technology Group, Industrial Technology Division, Malaysian Nuclear Agency, 43000 Kajang.

e-mail: ikn1000@nuclearmalaysia.gov.my

ABSTRACT

Thermoelectric nanostructures hold great promise for capturing and directly converting into electricity some vast amount of low-grade waste heats now being lost to the environment (e.g. from nuclear power plant, fossil fuel burning, automotives and household appliances). In this study, large-area vertically-aligned silicon nanowire (SiNW) arrays were synthesized in an aqueous solution containing AgNO_3 and HF on p-type Si (100) substrate by self-selective electroless etching process. The etching conditions were systematically varied in order to achieve different stages of nanowire formation. Diameters of the SiNWs obtained varied from approximately 50 to 200 nm and their lengths ranged from several to a few tens of μm . Te/ Bi_2Te_3 -Si thermoelectric core-shell nanostructures were subsequently obtained via galvanic displacement of SiNWs in acidic HF electrolytes containing HTeO_2^+ and $\text{Bi}^{3+}/\text{HTeO}_2^+$ ions. The reactions were basically a nano-electrochemical process due to the difference in redox potentials between the materials. The surface-modified SiNWs of core-shell structures had roughened surface morphologies and, therefore, higher surface-to-bulk ratios compared to unmodified SiNWs. They have potential applications in sensors, photovoltaic and thermoelectric nanodevices. Growth study on the SiNWs and core-shell nanostructures produced is presented using various microscopy, diffraction and probe-based techniques for microstructural, morphological and chemical characterizations.

ABSTRACT

Termoelektrik berstruktur nano memberi harapan yang cerah kerana ianya dapat menangkap dan secara terus menular kepada kuasa elektrikbeberapa jumlah luas sisa gred rendah menghangatkan sekarang sedang kalah kepada persekitaran (misalnya dari logi kuasa nuklear,bahan api fosil pembakaran, automotives dan peralatan rumahtangga). Dalam kajian ini, kawasan yang besar secara menegak menjajarkan silikon dawai nano (SiNW) kumpulanmensintesis dalam satu larutan berair mengandungi AgNO_3 and HF di Si yang jenis p (100) substrat oleh proses punar kurang elektrolis diri memilih. Syarat-syarat punaran secara sistematik diubah supayamencapai pelbagai peringkat pembentukan dawai nano. Garis pusat Si dawai nano memperolehi berbagai-bagai dari kira-kira 50 untuk 200 nm dan panjang mereka berjarak dari beberapa bagi beberapaberpuluh-puluh μm . Te / lapisan struktur nano Bi_2Te_3 -Si thermoelectriccore kemudiannya memperolehi melalui sesaranrangsang SiNWs dalam ELEKTROLIT HF berasid mengandungi HTeO_2^+ and $\text{Bi}^{3+} / \text{HTeO}_2^+$ ions. Reaksi-reaksi pada asasnya satunano proses elektrokimia disebabkan perbezaan dalam potensi-potensi redoks antara bahan-bahan. Permukaan mengubahsuai SiNWs lapisan struktur-struktur teras telah menggerutu permukaan morphologies dan oleh itu, permukaan yang lebih tinggi untuknisbah-nisbah pukal berbanding dengan SiNWs tanpa ubahsuai. Mereka mempunyai kegunaan yang berpotensi dalam pengesan-pengesan, fotovolta dan nanodevices termoelektrik. Kajian pertumbuhan di SiNWs dan lapisan struktur nano teras menghasilkan menyampaikan menggunakan berbagai-bagai mikroskopi, belauan dan teknik-teknik berasaskan kajian mikrostruktur kerana gambaran sifat morfologi dan kimia.

Keywords: Self-selective electroless etching, galvanic displacement, thermoelectric nanostructures.

INTRODUCTION

Semiconductor nanowires (NWs) have attracted much attentions owing to the unique electrical and optical properties they possess besides their potential applications as critical interconnect elements and basic building blocks in many areas of nanotechnology (Cui and Lieber, 2001). NWs are widely studied in recent years and much effort has been devoted to growing SiNWs with controlled morphology, chemistry, microstructures, localization and device structures (e.g. Schubert et. al., 2004). Among different growth methods used, chemical vapor deposition (CVD) based on vapor-liquid-solid (VLS) growth mechanism (Wagner and Ellis, 1964 and Ng et. al., 2011) has been the most established and widely used method for growing crystalline SiNWs as it provides good control over composition, size, crystallographic direction and location. SiNWs have also been grown via solid-liquid-solid (SLS) route under high temperature using Au-coated silicon substrate as catalyst (Chang et. al., 2006 and Ng et. al., 2011). The above techniques normally require one or more of the following factors for NW synthesis; high synthesis temperature, high vacuum environment, hazardous gas precursor and sophisticated instrumentation. To overcome these drawbacks, self-selective electroless etching based on localized electrochemical redox reactions has recently been proposed (Peng et. al., 2002). Self-selective electroless etching as proposed by Peng et al. (2002) is based on localized nano-electrochemical redox reactions and self-selective chemical etching process, where, in the case of $\text{AgNO}_3:\text{HF}:\text{Si}$ system, SiNW arrays and silver dendrite coatings are obtained on the Si substrate surface. Localized electroless metal deposition and selective etching take place simultaneously, through cathodic and anodic processes respectively, at the catalytic sites on the base substrate. Due to the preliminary nanowire formation mechanisms and their relationship with conventional electroless etching, this new technique is termed self-selective electroless etching. Subsequent studies on this technique have led to the proposal of possible mechanisms for nanowire formation (Qiu et. al., 2006).

EXPERIMENTAL

Regular substrates measuring approximately 20 x 15 mm were cut from polished high-grade p-type Si (001) wafers. The Si substrates were chemically cleaned using standard procedures and dried in a desiccator. After drying, the surface of each substrate was masked with a thin layer of insulating lacquer only to expose a fixed area measuring $\sim 10 \times 10$ mm. The substrates were then etched in an electrolyte bath containing an aqueous solution of 0.04 AgNO_3 and 5 M HF. The etching time was systematically varied between 15 - 120 minutes and the etching temperature ranged from room temperature to 50°C. The as-prepared samples were subsequently etched in 6 M HNO_3 to remove the dense silver dendrite overgrowths to reveal the arrays of well-aligned SiNWs underneath. The morphology, microstructure and chemistry of the silver dendrite overgrowths and the SiNWs obtained were characterized using scanning electron microscope (SEM), energy dispersive X-ray spectroscopy (EDX), transmission electron microscopy (TEM) and X-ray diffractometry (XRD). Te-Si and Bi_2Te_3 -Si core-shell structures were subsequently obtained by galvanic displacement of SiNWs in an acidic HF electrolyte containing HTeO_2^+ and $\text{Bi}^{3+}/\text{HTeO}_2^+$ ions respectively. This was done by immersing the SiNW arrays or free-standing SiNWs into 0.01 M of TeO_2 in 5 M HF or 0.01 M $\text{TeO}_2 + 0.008$ M $\text{Bi}(\text{NO}_3)_3 \cdot 5\text{H}_2\text{O}$ in 5 M HF, maintained at different temperatures for different durations.

RESULTS AND DISCUSSION

After the self-selective electroless etching process, the as-synthesized samples were initially covered with thick films of metallic silver particles and tree-like silver dendrite overgrowths as evident from the typical top-view SEM images of the samples in Fig. 1(a) and (b). Dendrite formation was more prominent and denser with increasing etching time as may be inferred by comparing the Ag/Si peak intensity ratios for the EDX traces in Fig. 1(a) and (b). The mechanism of silver dendrite formation has already been discussed in details by Qiu et.

al, (2006). Upon removal of the silver dendrite overgrowths using HNO_3 aqueous solution, large-area well-aligned SiNW arrays are seen self-assembled on the Si substrates as seen in Fig. 1(c) and (d). The SiNW arrays are of high chemical purity as shown by the EDX spectra in the inset of Fig. 1(c). Free-ends of the NWs tend to bundle into nanoclusters of increasing sizes as the lengths of the NWs grow with longer etching times.

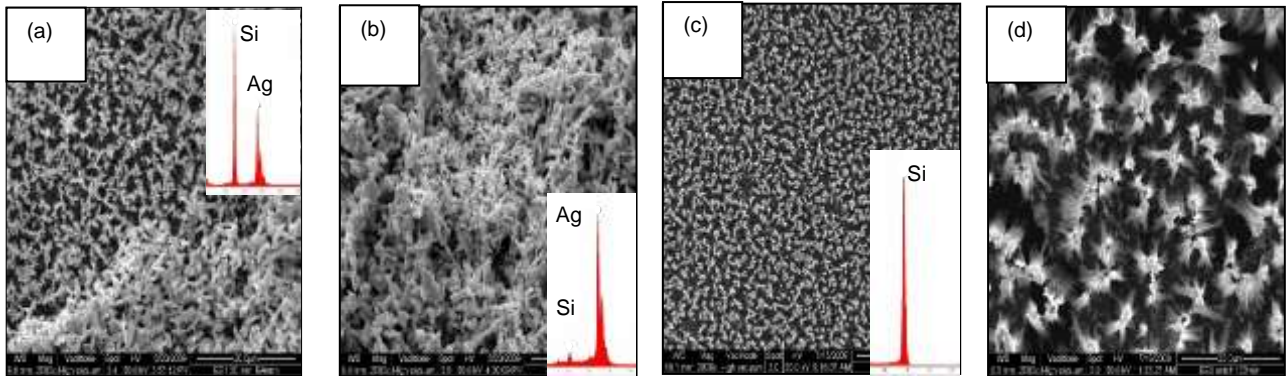


Fig. 1: Top-view SEM images. (a) and (b) Typical morphologies of the silver dendrite overgrowths for etching durations of 30 and 120 min. respectively. (c) and (d) The same samples, after removal of silver dendrite overgrowths, revealing dense SiNW arrays underneath.

Generally, the lengths of the NWs vary as a function of etching time and electrolyte temperature. Fig. 2(a) and (b) show, representatively, the cross-sectional SEM images of a series of SiNW arrays (etched at 40°C) for different etching durations. Fig. 2(c) and (d) are the representative cross-sectional SEM images from a series of SiNW arrays obtained at a fixed etching duration of 120 min but at different etching temperatures. Our SEM observations reveal that the length of the SiNW arrays increased steadily from ~ 10 to $40 \mu\text{m}$ when the etching time was increased from 30 to 120 minutes and from ~ 20 to $40 \mu\text{m}$ when the etching temperature was increased from room-temperature to 50°C .

Fig. 3(a) and (b) are the XRD spectra taken from the SiNW arrays before removing silver dendrite overgrowths. The Ag/Si peak intensity ratios increase with increasing density of the silver dendrite overgrowths, supporting the trend observed for EDX traces in Fig. 1(a) and (b). Fig. 3(c) is the XRD spectrum taken from the NW arrays after removing silver dendrite overgrowths. It can be observed that besides the strong 004 reflections from the substrate, weaker reflections arising from small dimensions of the SiNWs are indicative of their crystalline nature.

Fig. 4(a) is the TEM bright-field image of a single SiNW. Selected area diffraction pattern (SADP) in the inset shows that the NW is single-crystalline. HRTEM image of the NW in Fig. 4(b) shows a single-crystalline silicon core surrounded by an amorphous sheath which is most likely to be the native SiO_x formed due to extended air exposure after NW synthesis. Energy dispersive X-ray (EDX) spectroscopy performed on single SiNWs show no element other than Si and O could be traced along the NW, except for C which could be present as the impurity gas species in the TEM column (Fig. 5)

Te-Si and Bi_2Te_3 -Si core-shell structures were subsequently produced via post-growth modification of SiNWs. This was done by galvanically displacing SiNWs with Te or Bi_2Te_3 in an acidic HFelectrolyte containing HTeO_2^+ and $\text{Bi}^{3+}/\text{HTeO}_2^+$ ions respectively. This is an electrochemical process brought about by the difference in redox potentials between the materials. Representative SEM image in Fig. 4(c) shows an array of Te-Si core-shell structures on Si substrate obtained via the galvanic displacement process for 30 minutes at room-temperature. Fig. 4(d) shows a typical Bi_2Te_3 -Si core-shell structure obtained via the same process for 45 minutes at room temperature. The core-shell structures in both cases exhibit roughened surface morphologies. TEM image in Fig. 6(a) show a cluster of the Te-Si core-shell structures. The enlarged image of a single Te-Si core-shell structure in Fig. 6(b) shows that it is decorated with Te nanoparticles giving a thorn-like surface morphology which increases its surface area significantly. Selected area diffraction pattern (SADP) in the inset of Fig. 6(b) indicates the polycrystalline nature of the roughened Te outer layer. Roughened Te/ Bi_2Te_3 -Si NW core-shell structures have great potentials in non-reflecting, photovoltaic and thermoelectric applications.

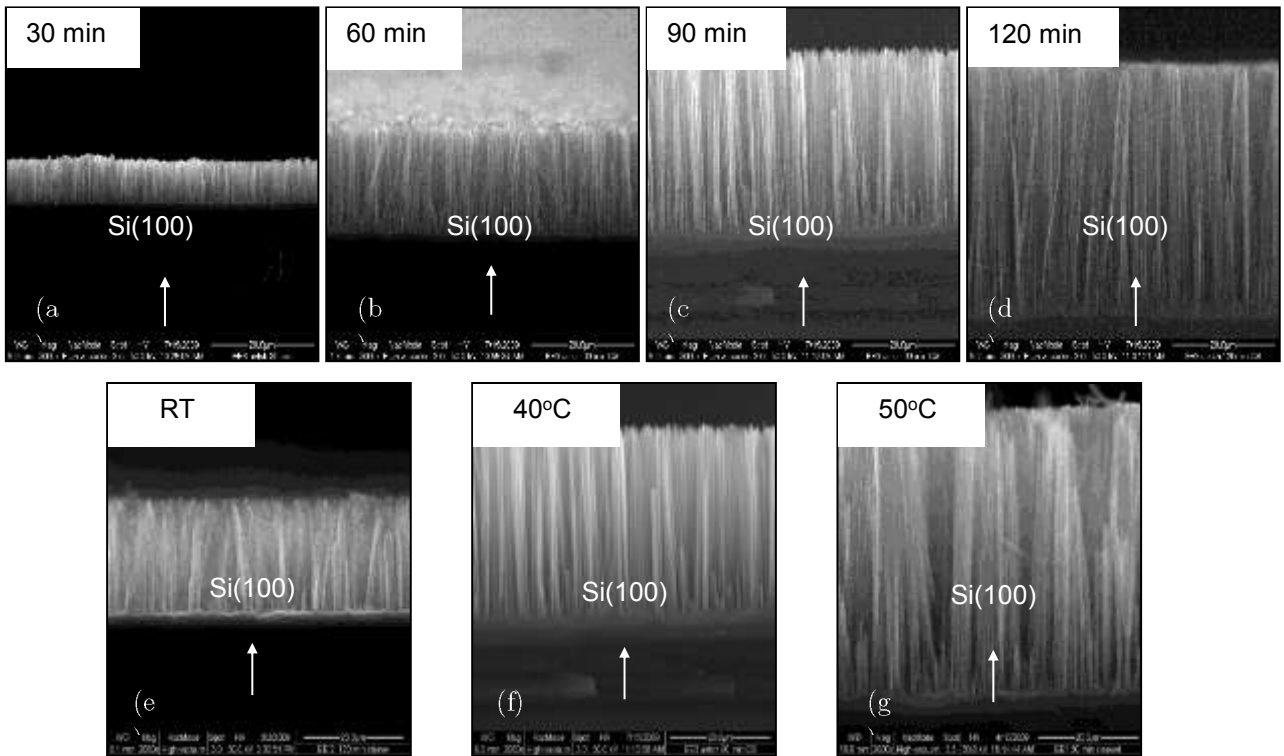


Fig. 2: Representative cross-sectional SEM images of the SiNW arrays. (a) to (d) NWs synthesized at 40°C showing variation in length as a function of etching time. (e) to (g) NWs etched for 120 min showing variation in length as a function of etching temperature.

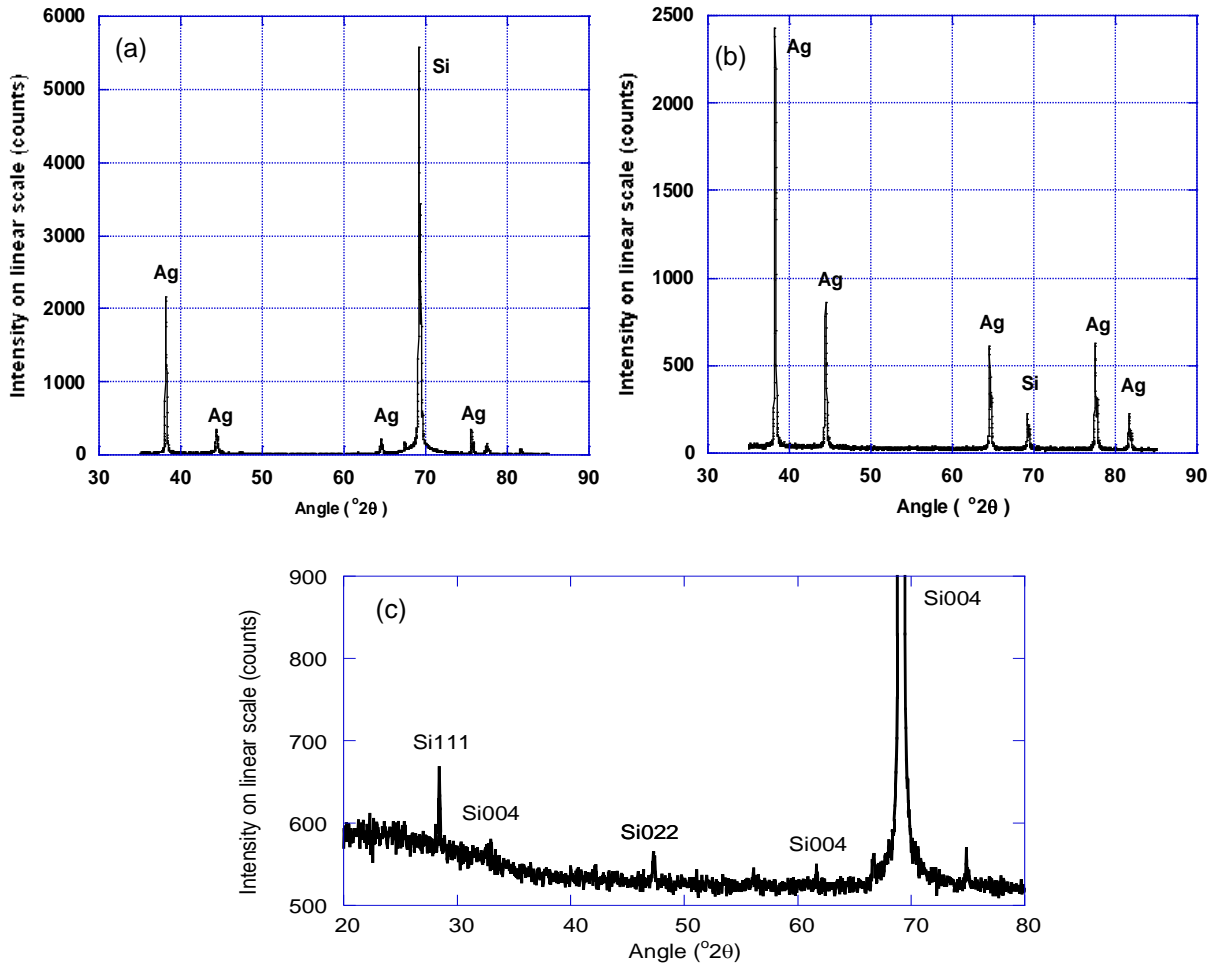


Fig. 3: (a) and (b) are the XRD spectra from SiNW samples which have been etched for (a) 30 min and (b) 120 min respectively, before removal of silver dendrite overgrowths. (c) XRD spectrum of the SiNW arrays after removal of silver dendrite overgrowths.

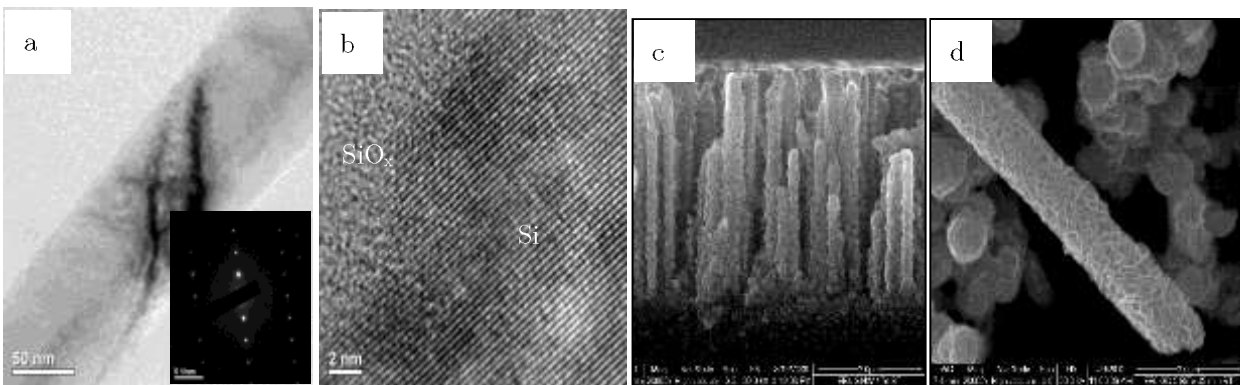


Fig. 4: (a) TEM bright-field image of a SiNW. Inset: The corresponding Si single-crystal diffraction pattern recorded from the NW. (b) HRTEM image of a section of the NW in (a) showing single crystalline Si core and amorphous SiO_x sheath. (c) and (d) SEM images of Te-Si and Bi₂Te₃-Si NW core-shell structures.



Fig. 5: Typical EDX spectrum recorded from a single Si nanowire. (The Cu peaks are from the TEM sample grid)

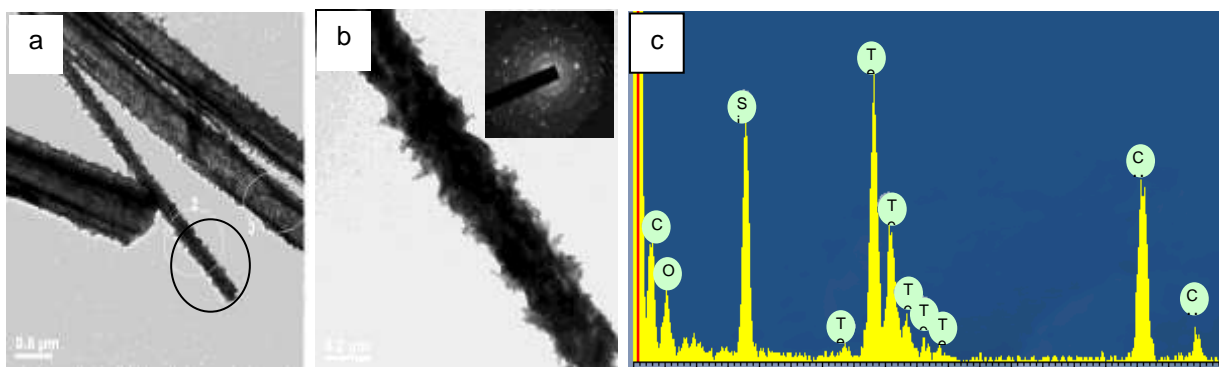


Fig. 6: TEM bright-field image of a cluster of Te-Si core-shell structures, (b) Magnified image from the circled region in (a) and (c) EDX spectrum from the Te-Si core-shell structure

CONCLUSION

The present study has demonstrated that vertically-aligned highly crystalline SiNW arrays have been successfully produced on Si (100) substrates via self-selective electroless etching. Selective lengths of the SiNWs produced were tunable by controlling the durations of the electroless etching process. Te/Bi₂Te₃-Si core-shell heterostructures were subsequently obtained through post-growth galvanically displacement SiNWs in acidic HF electrolytes containing HTeO₂⁺ and Bi³⁺/HTeO₂⁺ ions.

ACKNOWLEDGEMENT

The authors would like to acknowledge the Malaysian Government for funding this work (Science Fund Grant No: 03-03-01-SF0145).

REFERENCES

Chang, J. B., Liu, J. Z., Yan, P. X., Bai, L. F., Yan, Z. J., Yuan, X. M. and Yang, Q. (2006). Ultrafast Growth of Single-Crystalline Si Nanowires, *Mater. Lett.* 60, 2125 – 2128.

- Cui, Y. and Lieber, C. M. (2001), Functional Nanoscale Electronic Devices Assembled using Silicon Nanowire Building Blocks, *Science* 291, 851 – 853.
- Ng, I. K. and Suzuki, H. (2009). Low temperature growth of Si nanowires via vapour-liquid-solid mechanism. Materials Research Innovations, *Materials Research Innovations* 13 (3), 192 - 195.
- Ng, I. K., Kok, K. Y., Zainal Abidin, S. S., Saidin, N. U., Choo, T. F., Goh, B. T., Chong S. K. and Abdul Rahman, S. (2011). Gold catalysed growth of silicon nanowires and core-shell heterostructures via solid-liquid-solid process and galvanic displacement, *Materials Research Innovations* 15 (Suppl 2), 55 - 58.
- Peng, K. Q., Yan, Y. J., Gao, S. P. and Zhu, J. (2002). Synthesis of Large-Area Silicon Nanowire Arrays via Self-Assembling Nanoelectrochemistry, *Adv. Mater.* 14 (16), 1164 - 1167.
- Qiu, T., Wu, X. L., Siu, G. G. and Chu, P. K. (2006). Intergrowth Mechanism of Silicon Nanowires and Silver Dendrites, *J. of Electronic Mater.* 35 (10), 1879 - 1884.
- Schubert, L., Werner, P., Zakharov, N. D., Gerth, G., Kolb, F. M., Long, L., Gösel, U., Tan, T. Y. (2004). Silicon Nanowhiskers Grown on <111> Si Substrates by Molecular-Beam Epitaxy, *Appl. Phys. Lett.*, 84 (24), 4968 - 4970
- Wagner, R. S. and Ellis, W. C. (1964). Vapor-Liquid-Solid Mechanism of Single Crystal Growth, *Appl. Phys. Lett.* 4, 89 – 90.